
Research Article: New Research | Cognition and Behavior

Investigation of neural substrates of erroneous behavior in a delayed-response task

<https://doi.org/10.1523/ENEURO.0490-21.2022>

Cite as: eNeuro 2022; 10.1523/ENEURO.0490-21.2022

Received: 25 November 2021

Revised: 8 March 2022

Accepted: 24 March 2022

This Early Release article has been peer-reviewed and accepted, but has not been through the composition and copyediting processes. The final version may differ slightly in style or formatting and will contain links to any extended data.

Alerts: Sign up at www.eneuro.org/alerts to receive customized email alerts when the fully formatted version of this article is published.

Copyright © 2022 Chae et al.

This is an open-access article distributed under the terms of the Creative Commons Attribution 4.0 International license, which permits unrestricted use, distribution and reproduction in any medium provided that the original work is properly attributed.

1 **1. Manuscript Title:** Investigation of neural substrates of erroneous behavior in a delayed-
2 response task

3 **2. Abbreviated title:** Neural substrates of erroneous behavior

4 **3. Authors:** Soyoung Chae¹, Jeong-woo Sohn², Sung-Phil Kim¹

5 ¹ Department of Biomedical Engineering, Ulsan National Institute of Science and Technology,
6 50, UNIST-gil, Eonyang-eup, Ulju-gun, Ulsan, 44929, South Korea

7 ² Department of Medical Science, Catholic Kwandong University, International St. Mary's
8 Hospital, 24 Beomil-ro 579 beon-gil, Gangneung-si, Gangwon-do, 25601, South Korea

9 **4. Authors Contributions:** S. Chae designed research and analyzed data and S. Chae, J.-W.
10 Sohn and S.-P. Kim performed the research and wrote the paper

11 **5. Corresponding author:** Correspondence should be addressed to Sung-Phil Kim at
12 spkim@unist.ac.kr or Jeong-woo Sohn at jsohn@ish.ac.kr

13 **6. Number of Figures:** 9

14 **7. Number of Tables:** 0

15 **8. Number of Multimedia:** 0

16 **9. Number of words for Abstract:** 250

17 **10. Number of words for Significance Statement:** 120

18 **11. Number of words for Introduction:** 737

19 **12. Number of words for Discussion:** 1593

20 **13. Acknowledgements:** We especially thank the Svoboda laboratory for the generous
21 contribution of data publicly at <http://crens.org/>, a data-sharing website supported by NSF and

22 NIH, USA.

23 **14. Conflict of Interest:** Authors report no conflict of interest

24 **15. Funding sources:** This study was supported by the Brain Convergence Research Programs

25 of the National Research Foundation (NRF) funded by the Korean government (MSIT) (NRF-

26 2019M3E5D2A01058328, 2021M3E5D2A01019542).

27

28

29 **Title:** Investigation of neural substrates of erroneous behavior in a delayed-response task

30 **Abstract**

31 Motor cortical neurons exhibit persistent selective activities (selectivity) during motor planning.
32 Experimental perturbation of selectivity results in the failure of short-term memory retention
33 and consequent behavioral biases, demonstrating selectivity as a neural characteristic of
34 encoding previous sensory input or future action. However, even without experimental
35 manipulation, animals occasionally fail to maintain short-term memory leading to erroneous
36 choice. Here, we investigated neural substrates that lead to the incorrect formation of selectivity
37 during short-term memory. We analyzed neuronal activities in anterior lateral motor cortex
38 (ALM) of mice, a region known to be engaged in motor planning while mice performed the
39 tactile delayed-response task. We found that highly selective neurons lost their selectivity while
40 originally non-selective neurons showed selectivity during the error trials where mice licked
41 toward incorrect direction. We assumed that those alternations would reflect changes in
42 intrinsic properties of population activity. Thus, we estimated an intrinsic manifold shared by
43 neuronal population (*shared space*), using factor analysis and measured the association of
44 individual neurons with the shared space by communality, the variance of neuronal activity
45 accounted for by the shared space. We found a positive correlation between selectivity and
46 communality over ALM neurons, which disappeared in erroneous behavior. Notably, neurons
47 showing selectivity alternations between correct and incorrect licking also underwent
48 proportional changes in communality. Our results demonstrated that the extent to which an
49 ALM neuron is associated with the intrinsic manifolds of population activity may elucidate its
50 selectivity and that disruption of this association may alter selectivity, likely leading to
51 erroneous behavior.

52 **Significance Statement**

53 Appropriate retaining of short-term memory can maximize a future reward. During retention,
54 neurons in frontal cortex show persistent activity encoding a selection of future action, the
55 collapse of which leads to erroneous behavior. This study addressed the underlying neural
56 mechanism for changes of selectivity in erroneous behavior by investigating selectivity in
57 rodent anterior lateral motor cortex (ALM) during the delayed-response task. We found that
58 the stronger a neuron's activity was coupled to an intrinsic *shared space* of ALM, the greater
59 its selectivity was. Also, changes in selectivity during erroneous behavior were related to
60 changes in coupling strength. Our work suggests that proper association with the shared space
61 is key to orchestrating ALM neuronal activities for accurate planning for upcoming movement.

62 **Introduction**

63 Appropriate motor planning is essential to accurate motor control. Neurons in motor cortex
64 modulate their activity for motor planning before movement onset (Tanji and Evarts, 1976;
65 Weinrich et al., 1984). This preparatory activity contains information on forthcoming
66 movement such as reaction time (Riehle and Requin, 1989; Churchland and Shenoy, 2007).
67 Similar to motor cortical preparatory activity shown in non-human primates, anterior lateral
68 motor cortex (ALM), which is a central part of motor planning circuits in mouse, shows
69 selective firing activities (i.e., termed as selectivity) depending upon the direction of upcoming
70 movements (Li et al., 2015). Neural circuits involving ALM neurons that generate selectivity
71 during movement preparation have been investigated using a delayed-response task where a
72 sensory cue informs animals which direction to lick after delay (Chen et al., 2017; Guo et al.,
73 2017; Gao et al., 2018; Wang et al., 2021). For example, disruption of selectivity in ALM by
74 photoinhibiting relevant neural circuits leads to failure of short-term memory retention. Thus,
75 proper maintenance of selectivity is necessary for ALM to link past sensory cue and future
76 action.

77 Even after learning a delayed-response task, however, animals often perform the task
78 incorrectly without external perturbation. Such erroneous behavior is likely to be associated
79 with error in motor planning, potentially attributed to several hypothetical sources. For instance,
80 a received sensory cue could be misrepresented in neurons participating in movement
81 preparation (Panzeri et al., 2017). Or the stochastic nature of the evolution of neural states
82 underlying motor cortical activity can drive neural states toward a wrong subspace by chance
83 (Inagaki et al., 2019). While these accounts are plausible and worth exploring, a simpler starting
84 point to investigate neural substrates of erroneous behavior would be examining possible
85 sources that underpin changes in the selectivity of neurons, as selectivity has been shown to be

86 substantially disrupted when movement error ensues (Li et al., 2015) .

87 Therefore, the present study aims to investigate neural substrates of erroneous behavior in a
88 delayed-response task by focusing on neural determinants of the disruption of selectivity during
89 motor planning. To this end, we analyze ALM activity in three folds. First, at a single neuronal
90 level, we examine how the selectivity of single ALM neurons is disrupted for erroneous
91 behavior. Second, at a neuronal population level, we investigate if there is a collective pattern
92 in the disruption of selectivity by inspecting an intrinsic manifold shared by population (i.e.,
93 the *shared space*) (Athalye et al., 2017). We employ factor analysis (FA) to infer the shared
94 space from observed ALM population activity. Third, by integrating both single neuron and
95 population levels, we associate individual neuronal activities with the shared space and analyze
96 how these associations are altered during erroneous behavior. As FA allows the decomposition
97 of individual neuronal activities into shared and private signals (Athalye et al., 2017), where
98 the shared signal reflects the portion of a neuronal activity generated from latent factors in the
99 shared space, the analysis of the shared signal would reveal how disruption of population-level
100 activity connects to that of individual neuronal activity. Specifically, we investigate how the
101 selectivity of a single neuron is related to the shared space and whether such a relationship is
102 altered for erroneous behavior.

103 At the single neuronal level, we observed alternations in the selectivity during erroneous motor
104 planning. We observed a false drive of selective firings of ALM neurons, resulting in increases
105 in the selectivity of those neurons that were less selective in preparation of correct behavior
106 and vice versa. At the population level, we confirmed that movement direction information was
107 inadequately represented in the shared space during erroneous motor planning. Finally, by
108 associating the selectivity of single neurons with the shared space, we found that the selectivity
109 of single neurons was positively correlated with the variance of neuronal activity accounted for

110 by the shared space (i.e., termed as communality), which showed that neurons more strongly
111 tied to the shared space tended to exhibit greater selectivity. Such correlations disappeared
112 when the mice licked to the incorrect direction. We found that changes of selectivity from
113 correct to incorrect trials were positively correlated with changes of communality from correct
114 to incorrect trials during the delay period. It suggests that erroneous behavior may be caused
115 by both the decreased selectivity of originally more selective neurons and the increased
116 selectivity of originally less selective neurons, which seems to occur in relation to changes in
117 those neurons' coupling to the shared space, especially during motor planning.

118

119 **Materials and Methods**

120

121 **Datasets**

122 In this study, we analyzed two open datasets (Li et al., 2014; Chen et al., 2016) that contained
123 the same experimental data in a total of 38 mice (26 males and 12 females, ages > P60). Action
124 potentials (spikes) were simultaneously recorded in left ALM with silicon probes (part# A4x8-
125 5mm-100-200-177, NeuroNexus). The datasets are publicly available online at the
126 Collaborative Research in Computational Neuroscience website (<http://crcns.org>), contributed
127 by the Svoboda laboratory. A detailed description of the procedure to collect data can be found
128 in Li *et al.* (Li et al., 2015; Li et al., 2016). In brief, the mice were trained to sense the contact
129 position of a pole (anterior or posterior) in their whiskers to perform a tactile delayed-response
130 task (Fig. 1A). At the beginning of each trial of the task, a pole touched the whisker of the mice
131 for 1.3 seconds (sample period), cueing the direction of an upcoming reward (left or right).
132 After the pole was detached from the whisker, the mice waited for another 1.3 seconds (delay
133 period), then executed a licking movement (response period) (Fig. 1A). The mice received a
134 water reward if they licked to the right provided that the pole had touched the posterior part
135 (called a hit right (HR) trial), or to the left provided that it had touched the anterior part of the
136 whisker (called a hit left (HL) trial). A trial ended with no reward if the mice licked either to
137 the left given the posterior cue (called an error right (ER) trial) or to the right given the anterior
138 cue (called an error left (EL) trial) (Fig. 1B). On average, each mouse performed 4.84 sessions
139 for multiple days, where each session consisted of 100.43 trials of HR, HL, ER and EL.
140 Extracellular traces were recorded from left ALM and band-pass filtered (300 – 6,000 Hz). A
141 spike was extracted from the filtered trace by visual inspection with a spike width calculated
142 as a trough-to-peak interval in the average spike waveform (Guo et al., 2014). Units with spike

143 width < 0.35ms were defined as fast-spiking GABAergic (FS) neurons (196/2,420) and units
 144 with spike width > 0.45ms as putative pyramidal neurons (2,135/2,420). Units with
 145 intermediate values (0.35-0.45ms) were excluded from our analyses (89/2,420).

146

147 **Neuronal firing rates**

148 The firing rate of a neuron was calculated by counting spikes within a non-overlapping 100-
 149 ms bin. We also defined a firing rate change for each period (sample, delay, and response) as
 150 the mean firing rate in each period divided by the mean firing rate in baseline (0.3~0 s before
 151 tactile cue onset) (Fig. 1E). Note that no firing rate change was calculated for those neurons
 152 which did not fire during baseline.

153

154 **Selectivity**

155 ALM neurons reveal selectivity that characterizes differential firing rates depending on licking
 156 directions (Li et al., 2015; Li et al., 2016; Guo et al., 2017; Economo et al., 2018; Gao et al.,
 157 2018; Inagaki et al., 2018; Inagaki et al., 2019). We classified a neuron as ipsi-preferring if its
 158 firing rate was significantly higher in the HL than in the HR trials, contra-preferring if vice
 159 versa, or non-selective if no significant difference was found ($p < 0.01$, one-tailed Mann-
 160 Whitney test). We conducted this classification of neurons independently within each period.

161 We defined the selectivity of an ipsi-, or contra-preferring neuron in a given similar to the
 162 previous study (Inagaki et al., 2018):

$$\text{Selectivity} = 2 \times \frac{fr_{HR} - fr_{HL}}{\text{Max}(fr_{HR}) + \text{Max}(fr_{HL})} \quad (1)$$

163 where fr_{HR} (fr_{HL}) and $\text{Max}(fr_{HR})$ ($\text{Max}(fr_{HL})$) denote the mean and maximum firing rates across
 164 the HR trials (HL trials), respectively. From eq. (1), contra-preferring neurons should have

165 positive selectivity whereas ipsi-preferring neurons should have negative one. Normalization
166 in eq. (1) was necessary for generalizing and comparing the selectivity across neurons
167 regardless of sessions. In normalization, we divided the difference in firing rates between HR
168 and HL trials by maximum firing rate during HR and HL trials. Most of the selectivity had
169 value between -0.5~0.5, we multiplied two to set the selectivity value between -1~1. Note that
170 the maximum values are only for the period under consideration (sample, delay and respond
171 period each), and we used mean firing rate in the period (averaged across time points) and
172 calculated the selectivity.

173 Then, we estimated the selectivity of a neuron from data in the same way as the previous studies
174 (Li et al., 2015; Inagaki et al., 2018). Specifically, we randomly sampled firing rates from 30%
175 of the HR and HL trials and calculated $fr_{HR} - fr_{HL}$ in each period. We repeated this
176 calculation in eq. (1) 1,000 times and obtained the mean value, which was applied to eq. (1) to
177 compute selectivity. We also estimated the selectivity of a neuron in the error trials with the
178 same procedure, but by replacing the HR and HL with ER and EL trials, respectively (i.e.,
179 Neurons selective in ER: $fr_{ER} > fr_{HL}$). Note that we used Mann-Whitney test instead of t -
180 test to classify an ipsi-, or contra-preferring neuron in the error trials.

181

182 **Factor analysis**

183 We used factor analysis (FA) to infer a *shared space*, an intrinsic manifold shared by neuronal
184 population activity (Churchland et al., 2010; Everett, 2013; Athalye et al., 2017; Athalye et al.,
185 2018; Wei et al., 2019). Unlike other dimensionality reduction techniques such as principal
186 component analysis (PCA), FA focuses on finding latent variables (i.e., factors) that best
187 describe covariance between neurons (Byron et al., 2009; Athalye et al., 2017; Athalye et al.,

188 2018). Moreover, FA decomposes the firing activity of a neuron into a shared signal, which is
189 accounted for by population-shared latent variables, and a private signal, which is independent
190 of latent variables.

191 Before applying FA to population activity, we first trimmed firing activity data. So, to detect
192 and remove those neurons which did not exhibit action potentials due to unstable recordings,
193 we excluded neurons that were silent for more than 50% of the trials. After this process, the
194 data of 63 sessions in 22 mice out of 184 sessions in 38 mice were used for FA. We applied FA
195 to the firing rate data of a neuronal population in each period. As the previous study on the
196 same data showed that ALM neuronal firing activities during the delay period could be well
197 represented on a two-dimensional space (Inagaki et al., 2018), we also determined the number
198 of factors as two in our analyses. The previous study on the same task paradigm showed that
199 two modes capture over 60% across-trial variance in ALM activities. (Inagaki et al., 2018). We
200 calculated the mean variance explained by principal components after 100 random subsampling
201 of hit trials to match the number of hit trials and the number of error trials. We observed two
202 principal components explained similar level of variance of our data both in the hit and error
203 trials (hit trials, sample: $62.22 \pm 0.0069\%$, delay: $65.35 \pm 0.0056\%$, response: $64.34 \pm$
204 0.0067% mean \pm SEM across subsampling iterations; error trials, sample: $61.55 \pm 1.40\%$,
205 delay: $64.19 \pm 1.50\%$, response: $62.84 \pm 1.35\%$; mean \pm SEM across sessions). Note that
206 mean variance explained in the hit trials is mean of variance explained across iterations of
207 subsampling the hit trials. Because mean variance explained is over 60% regardless of
208 behavioral results (hit and error) and periods (sample, delay and response), we decided to fix
209 K as two.

210 A specific procedure to conduct FA on ALM data is as follows. Let $x \in R^N$ be a vector of the
211 firing rates of N neurons and $z \in R^k$ be a K -dimensional random vector ($K < N$) following a

212 multivariate normal distribution such as:

$$z \sim N(0, I) \quad (2)$$

213 FA assumes that x is generated from z by a linear model:

$$x \sim N(\mu + Uz, UU^T + \psi) \quad (3)$$

214 where $\mu \in R^N$ is a vector of the mean firing rates of N neurons, $U \in R^{N \times k}$ is a factor loading
 215 matrix illustrating a generative relationship from z to x and $\psi \in R^{N \times N}$ is a covariance matrix
 216 of residuals. We form a vector of the shared signals of N neurons, $x^{shared} = Uz$, and that of
 217 the private signals of N neurons $x^{private} = x - \mu - Uz$. Each vector follows a multivariate
 218 normal distribution:

$$x^{shared} \sim N(0, \Sigma^{shared}) \quad (4)$$

$$x^{private} \sim N(0, \Sigma^{private}) \quad (5)$$

219 where $\Sigma^{shared} = UU^T$ and $\Sigma^{private} = \Psi$. We can decompose x and its covariance as:

$$x = \mu + x^{private} + x^{shared} \quad (6)$$

$$\Sigma^{total} = \Sigma^{private} + \Sigma^{shared} \quad (7)$$

220 where Σ^{total} denotes the covariance matrix of x . The factor loading matrix U is estimated by
 221 the expectation-maximization (EM) algorithm (Dempster et al., 1977; Athalye et al., 2017;
 222 Athalye et al., 2018).

223

224 **Representation of licking directions in the shared space**

225 We evaluated the representation of licking directional information in the shared space. Let Z

226 be the matrix of the factor scores from every hit trial, $Z \in \mathbb{R}^{T \times K}$, where T is the number of the
 227 hit trials, including both the HR and HL trials and K is the number of factors. We assigned a
 228 factor score vector of each trial (i.e., each row of Z) to one of the two clusters corresponding to
 229 the licking direction. Then, we measured how well the two clusters were separated using the
 230 Fisher ratio (FR) given by:

$$\text{FR}(\text{LV1}_{\text{HR}}, \text{LV1}_{\text{HL}}) = \frac{(E[\text{LV1}]_{\text{HR}} - E[\text{LV1}]_{\text{HL}})^2}{\text{Var}[\text{LV1}]_{\text{HR}} + \text{Var}[\text{LV1}]_{\text{HL}}} \quad (8)$$

231 where LV1 is the first latent variable (i.e., the first factor) and $E[\cdot]_{\text{HR/HL}}$ and $\text{Var}[\cdot]_{\text{HR/HL}}$ represent
 232 its expected value and variance over the HR/HL trials, respectively. We also calculated the
 233 $\text{FR}(\text{LV2}_{\text{HR}}, \text{LV2}_{\text{HL}})$ for the second latent variable (LV2, the second factor) in the same way.
 234 The higher the FR is, the more the two clusters are separated. We repeated the same separability
 235 analysis for the error trials, where we assigned each factor score vector to one of the two
 236 clusters corresponding to the tactile cue instead of actual licking direction.

237 To establish a statistical criterion for determining if the latent variables contained licking
 238 directional information, we calculated a random FR by randomizing directional information.
 239 We shuffled directional information of all the hit trials, clustered latent variables accordingly,
 240 and measured the FR between the clusters. We repeated this procedure multiple times to
 241 establish a distribution of the random FR (Fig. 3B).

242 We validated the reliability of licking directional representations in the shared space via a train-
 243 and-test scheme. In this scheme, we first built a shared space using the first half of the hit trials
 244 such that the first half was used as training data. Then, we projected the firing rate data of the
 245 second half of the hit trials or those of the error trials onto that shared space such that these
 246 remaining data were used as testing data. The projection of a testing firing rate vector of the
 247 second half of the hit trials or the error trials, x , onto the shared space was conducted by

248 estimating a corresponding shared signal (\hat{x}^{shared}) and a factor score vector (\hat{z}) as (Athalye et
 249 al., 2017):

$$\hat{x}^{shared} = E[x^{shared}|x] = E[Uz|x] = UU^T(UU^T + \psi)^{-1}(x - \mu) \quad (9)$$

$$\hat{z} = (U^T U)^{-1} U^T \hat{x}^{shared} \quad (10)$$

250 where μ , U and ψ were estimated from the training data. Here, we denote a set of estimated
 251 factor score vectors from the second half of the hit trials as HIT_{test} and that from the error trials
 252 as ERR_{test} . We also repeated the same projection using the training data and denote a set of
 253 factor score vectors from the first half of hit trials as HIT_{train} .

254 Then, we measured a similarity between HIT_{train} and HIT_{test} or between HIT_{train} and ERR_{test} to
 255 assess the reliability of directional representations in the shared space. To this end, we divided
 256 the factor score vectors in each of HIT_{train} , HIT_{test} , and ERR_{test} into two clusters, respectively,
 257 according to the cue information (i.e., cued direction) (Fig. 3C). Then, we calculated the FR
 258 between the two clusters of HIT_{train} and HIT_{test} or HIT_{train} and ERR_{test} , that were assigned to
 259 the same cue (Fig. 3C, left). Similarly, we calculated the FR between the clusters assigned to
 260 the opposite cue (Fig. 3C, right). If the shared space remained consistent between training and
 261 testing, HIT_{train} and HIT_{test} would form similar clusters and the two clusters assigned to the
 262 same cue would be overlapped, resulting in a smaller FR. On the other hand, the two clusters
 263 assigned to the opposite cue would be apart from each other with a larger FR. We also examined
 264 whether this examination was held for ERR_{test} . For reference, we calculated the FR between
 265 the two clusters of HIT_{train} and compared other FR values to it. Pairwise comparisons between
 266 the reference and the other four FR values were performed: 1) $FR(HIT_{train}, HIT_{test})$ for same
 267 cue, 2) $FR(HIT_{train}, HIT_{test})$ for opposite, 3) $FR(HIT_{train}, ERR_{test})$ for same and 4) $FR(HIT_{train},$
 268 $ERR_{test})$ for opposite.

269

270 Selectivity of shared signals

271 To investigate whether the shared signal of each ALM neuron exhibited selectivity, we
272 estimated selectivity of shared signals in the same way as firing rates (see above), by replacing
273 firing rates in eq. (1) with shared signals, x^{shared} . Hereafter, we denote the selectivity of the
274 shared signal of a neuron as Sel_{SH} .

275

276 Reversed firing modulation with erroneous behavior

277 We assessed whether the selectivity of ALM neurons vanished or was reversed for erroneous
278 behavior by comparing individual neuronal firing activities between the error trials and the hit
279 trials. Among ipsi-, or contra-preferring neurons, we examined if there existed neurons that
280 reversed their firing modulation with erroneous behavior by showing significantly higher firing
281 rates in a non-preferred cue trial than in a preferred cue trial during the erroneous behavior
282 (Mann-Whitney test, $p < 0.05$).

283 Then, we examined whether such neurons reversed their firing rates together with other
284 neurons or independently during the task. To this end, we calculated trial-by-trial correlations
285 between the firing rates of all possible pairs of those neurons which showed reversed firing
286 modulation, in each of the error trials and the hit trials. Then, we evaluated whether correlations
287 were different or not between the hit and error trials using Wilcoxon signed-rank test. If the
288 correlations in the error trials remained unchanged compared to the hit trials, it would indicate
289 that the neurons reversed firing modulation collectively during the error trials.

290

291 **Analysis of generative relations from latent variables to shared signals**

292 We further analyzed how a generative relation from latent variables to the shared signals of
293 individual neurons was altered between the hit and error trials. Since this generative relation,
294 described by the factor loading matrix (U), could be altered by changes in U , changes in latent
295 variables (z), or changes in both U and z , we examined the effect of U or z on the selectivity
296 of shared signals (Sel_{SH}). To this end, we reconstructed shared signals in two ways. First, we
297 reconstructed shared signals through $x^{shared} = Uz$ with U estimated using the data in the
298 hit trials and z inferred using the data in the error trials. Second, we repeated the same
299 reconstruction with U estimated using the error trials and z inferred using the hit trials. In each
300 session, we calculated selectivity of shared signals reconstructed in either the first or the second
301 way above (reconstructed Sel_{SH}). We also calculated selectivity of shared signals originally
302 generated using the data in the hit trials (original Sel_{SH}). Collecting these selectivity values
303 from all sessions, we calculated correlations between original Sel_{SH} and reconstructed Sel_{SH}
304 for each way of reconstruction. If reconstructed Sel_{SH} in the first way was positively correlated
305 with original Sel_{SH} , it would indicate that z remained similar across the hit and error trials and
306 possible changes in selectivity of neurons might be attributed to changes in U . On the other
307 hand, if reconstructed Sel_{SH} in the second way was positively correlated with original Sel_{SH} , it
308 would indicate that U remained relatively similar across the hit and error trials and possible
309 changes in selectivity of neurons might be attributed to changes in z .

310

311 **Communality**

312 We employed communality as a metric to measure how much the firing activity of a single
313 neuron was explained by the shared space. Specifically, the communality of a neuron was

314 calculated as the sum of squared factor loadings associated with the neuron, thus representing
315 how much variance of the neuron's firing rate was accounted for by the latent variables. The i^{th}
316 neuron's communality was calculated by:

$$\text{Communality}_{\text{neuron}_i} = u_{i1}^2 + u_{i2}^2 \quad (12)$$

317 where u_{i1} and u_{i2} constitute the i^{th} row of the factor loading matrix U in eq. (3).

318 After calculating the communality of every neuron, we assessed a relationship between the
319 selectivity and communality of individual neurons using the linear regression analysis, where
320 a dependent variable and an independent variable were the selectivity and communality of each
321 neuron, respectively. Statistical significance of linear regression was evaluated by the F-test.

322

323 **Results**

324

325 **ALM neuronal selectivity changed when mice licked to wrong direction**

326 We first verified that a success rate of the tactile delayed-response task was not different
327 between licking directions across the sessions selected for FA (63 sessions): the mean and
328 standard error of the success rate was 79.17 ± 0.08 % for the HR trials and 75.18 ± 0.15 % for
329 the HL trials, respectively (Fig. 1C, $p = 0.28$, two-tailed paired t -test).

330 During the task, many ALM neurons showed selectivity in specific periods (see examples in
331 Fig. 1D). While the firing rates of selective neurons were obviously higher for their preferred
332 cue than non-preferred ones in the hit trials (Fig. 1E, left), such differences were largely absent
333 in the error trials (Fig. 1E, right). Notably, the firing rates of ipsi-preferring neurons were even
334 higher in the ER than in the EL trials during the response period (Fig. 1E, right).

335 Next, we inspected changes of selectivity between the hit and error trials. The Kolmogorov-
336 Smirnov test (K-S test) revealed no significant difference in the overall distributions of
337 selectivity between the hit and error trials (Fig. 2A, $ps > 0.05$ for every period). Thus, it
338 confirmed that selectivity did not disappear during the error trials. Rather, we observed that
339 neurons with higher selectivity in the hit trials tended to show reduced selectivity in the error
340 trials whereas those with lower selectivity in the hit trials tended to show increased selectivity
341 in the error trials (Fig. 2A). To examine these observations, we selected neurons showing
342 selectivity within the top (showing high selectivity in HR trials) and bottom (showing high
343 selectivity in HL trials) 5% of the selectivity distribution in the hit trials and tracked their
344 selectivity in the error trials. The absolute values of selectivity of these neurons significantly
345 decreased from the hit to error trials (Fig. 2B, $ps < 10^{-6}$ for every period, one-tailed paired t -
346 test). Similarly, we conducted the same analysis in the opposite direction – selecting neurons

347 with the top (showing selectivity in ER trials) and bottom (showing selectivity in EL trials) 5%
348 selectivity in the error trials and tracking their selectivity in the hit trials – and observed
349 significant decreases of the absolute selectivity from the error to hit trials (Fig. 2C, $ps < 0.01$
350 for every period, one-tailed paired t -test). We found that neurons selective during the hit trials
351 decreased their selectivity in the error trials ($ps < 0.01$ for every period, one-tailed paired t -test)
352 and neurons selective during the error trials also decreased selectivity in the hit trials ($ps < 0.05$
353 for every period, one-tailed paired t -test). Thus, relatively less selective neurons during the hit
354 trials could gain more selectivity during the error trials, indicating that those neurons that were
355 significantly selective during the hit trials decreased selectivity during the error trials, and those
356 neurons that were significantly selective during the error trials also decreased selectivity during
357 the hit trials. We explored this pattern in terms of neuronal relations to the shared space in the
358 following analyses.

359

360 **Reversed firing modulation with erroneous behavior**

361 We inspected if there was a set of neurons collectively showing reversed firing modulation
362 between the error and the hit trials (see the definition of reversed firing modulation in Methods),
363 as conceptually illustrated in Fig. 3A (e.g., contra-preferring neuron in the hit trials changes to
364 ipsi-preferring neuron in the error trials). In effect, among selective neurons, some neurons
365 jointly showed reversed firing rate modulation in the error trials and such joint reversal of firing
366 modulation disappeared when directional information was shuffled across the neurons (see Fig.
367 3B for example). We calculated pairwise correlations between neurons showing reversed firing
368 modulation in contra- and ipsi-preferring neurons respectively. Note that we pooled the
369 correlation coefficients of contra- and ipsi-preferring neurons together and conducted statistical
370 test due to small number of sample size. As a result, we found that the correlation coefficients

371 of neurons showing reversed remained unchanged or even greater in the error trials ($p < 0.05$
372 in sample; $ps > 0.05$ in delay and response period, sign rank-test) (Fig. 3C). These results
373 support that the selectivity was reversed in a number of ALM neurons followed by behavioral
374 error.

375

376 **Representation of licking directions in the shared space was disrupted for erroneous**
377 **behavior**

378 To investigate if ALM neuronal population represents task-related information together, we
379 estimated a 2D shared space of the firing rates of ALM neuronal populations using FA. We
380 could identify latent variables (i.e., factors) that best describe covariance matrix between
381 population of neurons through FA. Since two principal components capture over the majority
382 of variance (>60%) of data in every period of the hit and error trials, the number of latent
383 variables was fixed to two. Although the shared space was estimated solely from neuronal data
384 in an unsupervised way, we observed that task-related information (i.e., cued licking direction)
385 was present in the shared space (Fig. 4A, top). The Fisher ratio (FR) between the two clusters
386 in the shared space formed based on the cue information (i.e., HR vs. HL, or ER vs. EL) showed
387 a significant difference between the hit, error, and shuffled trials ($ps < 0.05$ for every period
388 and latent variable, one-way ANOVA, Fig. 4B). A *post-hoc* analysis showed that the FR of the
389 hit trials was greater than that of the shuffled trials in every period for both latent variables
390 except in the sample period for the second latent variable. However, the FR of the error trials
391 was greater than that of the shuffled trials only in the sample period ($p < 0.01$, Bonferroni-
392 corrected *post-hoc t*-test, Fig. 4B). Besides, it showed that the FR of the hit trials was greater
393 than that of the error trials in the response period on the first latent variable ($p < 0.01$). Thus,
394 in the hit trials, the cue information was separately represented in the shared space, which

395 became less distinguishable in the error trials.

396 Next, we tested the reliability of this representation of task-related information in the shared
397 space via a train-and-test scheme (see Methods). We constructed the shared space using the
398 first half of the hit trials. The second half of the hit trials and the error trials were projected on
399 the built shared space and measured FR to test if the directional information is still separated
400 on the shared space. If emergent shared space has consistent axes across trials, then FR of test
401 data would show FR values similar to those projected by the train data. The shared space built
402 from the first half of the hit trials consistently maintained a discriminative spatial pattern for
403 the second half of the hit trials projected onto that shared space (Fig. 4D, middle). In contrast,
404 the projection of the error trials onto the same shared space did not show a discriminative spatial
405 pattern clearly (Fig. 4D, bottom). Using the FR, we assessed the similarity of clustering patterns
406 in the shared space across the hit and error trials (see Methods). Between the two clusters across
407 the first and second halves of the hit trials corresponding to the same cue (Fig. 4C, left), the FR
408 was significantly reduced compared to original FR of the first half of the hit trials for every
409 period ($ps < 0.05$, one-tailed paired t -test), showing that the clusters assigned to the same cue
410 remained largely unchanged across the hit trials (Fig. 4E). In contrast, the FR with the opposite
411 cue (Fig. 4C, right) showed no difference from the reference value except for the second latent
412 variable during the sample period, showing that distinct representations of licking directions
413 were maintained across the hit trials. Between the hit and error trials ($HIT_{train} - ERR_{test}$), the FR
414 was largely reduced in the error trials with both the same and the opposite cue ($p < 0.05$, one-
415 tailed paired t -test) (Fig. 4E), showing that task-related information in the error trial was not
416 represented as clearly as in the hit trials. Moreover, the FR reduced more with the opposite cue
417 than with the same cue in the delay and response periods of the error trials ($p < 0.01$, one-tailed
418 paired t -test), which indicated that clustering patterns in the error trials appeared to be relatively

419 closer to those in the hit trials if licking directions were switched.

420

421 **ALM neurons showed selectivity in the shared signals**

422 In this section, we investigated how the selectivity of individual neurons was related to the
423 shared space and whether such a relationship was altered for erroneous behavior. By
424 decomposing the firing rate of a neuron into shared signals and private signals using FA (see
425 Methods), we analyzed the shared signals that reflected how the neuronal firing rate was
426 modulated by the shared space (see Methods). Of a total of 634 recorded ALM neurons, we
427 observed 220 contra-preferring neurons and 271 ipsi-preferring neurons (FR+, Fig. 5A).
428 Among these selective neurons, 107 contra-preferring neurons (48.6%) and 159 ipsi-preferring
429 neurons (58.7%) also showed selectivity in their shared signals (FR+SH+, Fig. 5A). We
430 focused on these FR+SH+ neurons, in which task-related information in the shared space was
431 reflected on the firing rate. Next, we compared the magnitudes of selectivity between the firing
432 rates and shared signals of the FR+SH+ neurons. We found that the selectivity of shared signals
433 (S_{SH}) was significantly greater than that of firing rates (Fig. 5B, top, $p_s < 0.05$ for every period,
434 one-tailed paired t -test). A linear regression analysis with S_{SH} as an independent variable and
435 that of firing rates as a dependent variable showed a significant linear relationship with slopes
436 less than 1 (Fig. 5B, bottom, $p_s < 0.01$). The result supports our assumption on a generative
437 relation of firing rates from latent variables that the selectivity of a single neuron may be related
438 to the shared space composed by population activity.

439 From the observed changes in firing rates (Fig. 2A, B) and latent variable patterns (Fig. 4A, D)
440 across the hit and the error trials, we examined how firing modulation of selective neurons was
441 altered during the error trials. In the perspective of a generative model (FA), if latent variables
442 in the error trials represent licking direction contrary to the direction that they should have

443 represented while the generative relationship described in the factor loading matrix remains
444 unchanged, the shared signal of selective neurons that are generated from the latent variables
445 should also exhibit selectivity in an opposite way to the hit trials.

446 Since this collectively reversed firing modulation indicated that the altered selectivity of ALM
447 neurons in the error trials might be driven by changes in the shared space, rather than an
448 independent change of modulation in individual neurons, we analyzed the possible changes in
449 the generation of shared signals from latent variables during the error trials. On one hand, when
450 we generated shared signals from latent variables using the error trials while keeping the factor
451 loading matrix (U), their selectivity became uncorrelated with their original selectivity obtained
452 from the hit trials in the sample and response periods, or even negatively correlated in delay
453 period ($r = -0.33$) (Fig. 6A). On the other hand, if we generated shared signals using U
454 estimated from the error trials while keeping latent variables, their selectivity was positively
455 correlated with their original selectivity in every period ($r = 0.68$ for the sample, $r = 0.68$ for
456 the delay, and $r = 0.79$ for the response period) (Fig. 6B). Hence, we confirmed that latent
457 variables were altered during the error trials rather than overall generative relationships from
458 latent variables to shared signals.

459

460 **ALM neuronal selectivity is correlated with communality**

461 For each neuron, we measured communality to determine how well the neuron's firing rate was
462 accounted for by the first two latent variables. Then, we examined a correlation between the
463 magnitude of selectivity and that of communality of the FR+SH+ neurons. For the hit trials,
464 we found significant positive correlations between communality and selectivity in every period
465 (sample: $r = 0.39$; delay: $r = 0.47$; response: $r = 0.47$; $ps < 0.01$ for every period) (Fig. 7A-B).

466 It revealed that the ALM neurons tended to be more selective when their firing rate modulation
467 contributed more to the shared space. However, such linear relationships disappeared in the
468 error trials (sample: $r = 0.06$; delay: $r = -0.11$; response: $r = 0.14$; $ps > 0.05$ for every period)
469 (Fig. 7C-D), implying that selective modulation of firing rates in the ALM neurons became
470 irrelevant to their dependency on the shared space in erroneous behavior especially during
471 movement preparation.

472

473 **Changes in selectivity between the hit and error trials were correlated with changes in**
474 **communality**

475 To understand why correlations between selectivity and communality present in the hit trials
476 disappeared in the error trials, we first compared overall distributions of communality between
477 the hit and error trials. The K-S test showed that cumulative density function of communality
478 in the hit trials was smaller than that in the error trials (Fig. 8A, $ps < 10^{-4}$ for every period).
479 However, we observed a similar pattern in communality changes between the hit and error
480 trials (Fig. 7B) as in selectivity (Fig. 2B) – neurons with higher communality in the hit trials
481 tended to reduce their communality in the error trials whereas those with lower communality
482 in the hit trials increased their communality in the error trials. To examine these observations,
483 we examined neurons with the top 10 % communality in the hit trials and found that they
484 significantly decreased communality in the error trials and vice versa (Fig. 8B-C, $ps < 0.01$ for
485 every period, one-tailed paired t -test).

486 Upon finding this similarity between selectivity and communality, we further investigated
487 whether neuron-level alterations in selectivity were related to those in communality. Although
488 we did not directly estimate the shared space from the selectivity, the task-related activities
489 would be captured in the shared space through covariance structure. Therefore, to identify a

490 specific aspect of dependency related to behavior in the shared space, we evaluated if each
491 neuronal engagement on the shared space could explain the selectivity and accounted for the
492 change in the selectivity in the error trials by changes in engagement on constructing the shared
493 space. Specifically, we tested if the amount of change of selectivity from the hit to error trials
494 would be explained by that of communality. To this end, we defined a change in communality
495 and selectivity of a neuron between the hit and error trials as $\Delta\text{com} = \text{communality}_{\text{Hit}} -$
496 $\text{communality}_{\text{Error}}$ and $\Delta\text{sel} = \text{selectivity}_{\text{Hit}} - \text{selectivity}_{\text{Error}}$, respectively, and performed a
497 correlation analysis between Δsel and Δcom in each period. The result showed relatively weak
498 but significant linear relationships between Δsel and Δcom across individual neurons (sample:
499 $r = 0.29, p < 0.05$; delay: $r = 0.27, p < 0.01$; response: $r = 0.33, p < 10^{-6}$). However, when we
500 performed the correlation analysis at the population level, where Δcom (or Δsel) was averaged
501 over a population of ALM neurons within each session, we found a stronger correlation
502 between Δcom and Δsel in the delay period ($r = 0.57, p < 10^{-3}$), but not in other periods (sample:
503 $r = 0.15, p = 0.52$; response: $r = 0.03, p = 0.81$) (Fig. 9A, B). The results suggest that changes
504 in single neurons' selectivity underlying erroneous behavior – i.e., the decreased selectivity of
505 originally more selective neurons and the increased selectivity of originally less selective
506 neurons – might occur in relation to changes in those neurons' communality, especially during
507 a motor planning period.

508 **Discussion**

509 The present study investigated neural substrates of erroneous behavior in rodents' ALM
510 populations during the tactile delayed-response task. Compared to correct behavior, the
511 selectivity of individual ALM neurons was reversed. Licking direction was inadequately
512 represented in the shared space by population, and connections of the selectivity of individual
513 neurons to the shared space, measured by correlations between selectivity and communality,
514 was disrupted, during erroneous behavior. Notably, average selectivity in animals changed
515 more between correct and erroneous behavior when the corresponding average communality
516 changed more, during the delay period. Our results suggest neural substrates of erroneous
517 behavior in the tactile delayed-task as joint changes in the selectivity of ALM neurons at both
518 single neuron and population levels, as well as alternation of the neuronal coupling assignment
519 to the shared space.

520 One of the intriguing findings of the present study was that the single neuron-level change in
521 selectivity between correct and erroneous behavior was highly correlated with the population-
522 level change in communality, which was observed only in the delay period. Also, we
523 demonstrated that highly selective neurons for correct behavior decreased their selectivity for
524 erroneous behavior whereas less selective neurons for correct behavior became more selective
525 for erroneous behavior. Together, significant alterations in selectivity of ALM neurons that
526 underlie erroneous behavior were tightly linked to changes in communality during the delay
527 period. Considering that changes of communality mean changes of the degree to which a
528 neuron's activity is coupled to the shared space, our results suggest that incorrect modulation
529 of ALM neurons that are less selective during movement preparation would be engaged in
530 causing behavioral error as supported by changes in selectivity.

531 Individual neuronal activities vary in part with those of other neurons, which creates "common

532 variance” shared among a number of neurons. Existence of such shared variance among
533 neurons enables us to find a low-dimensional space mathematically in which each dimension
534 represents co-varying activity of a subset of neurons in the population. If the shared variance
535 changes with the task, the task-related information would also be represented on the shared
536 space. In this study, we confirmed that future licking direction was discriminately represented
537 on the shared space for correct behavior but not for erroneous behavior. This implied that co-
538 varying activity of a subset of neurons in the population was not correctly coordinated for
539 erroneous behavior, indicating a possible error in the interaction between those neurons.

540 Moreover, stronger coupling of a single neuron to the shared space means that the neuron’s
541 activity is explained more by co-varying activity of a set of neurons that share variance. It
542 implies that a strongly coupled neuron might participate more in generating co-varying activity
543 pattern in the shared group. As it is known that selectivity is key to movement preparation, we
544 can assume that tight coupling of highly selective neurons sharing the same preferred direction
545 (i.e., contra-, or ipsi-preferring) would be important to make correct movements. We observed
546 that highly selective neurons showed stronger coupling to the shared space for correct behavior
547 and that these neurons reduced their coupling as well as selectivity for erroneous behavior.
548 Interestingly, we rather found that a different group of neurons that showed low selectivity for
549 correct behavior became more selective for erroneous behavior along with stronger coupling.
550 It indicates that a wrong set of neurons became more interactive during movement preparation
551 for erroneous behavior while the originally selective neurons were not properly coordinated.
552 Note that this wrong set of neurons partially involved selective neurons of opposite preferred
553 direction but mostly included neurons that had been non-selective if behaved correctly. It
554 implies that erroneous behavior might not be a consequence of wrong sampling of tactile cue,
555 which would have increased coupling of neurons of opposite preferred direction, but rather

556 involve more complicated processes of neuronal interactions in the ALM circuit which remains
557 vague and needs further in-depth investigations.

558 Although much more work should be needed to answer why changes in selectivity were
559 correlated with changes in communality only during the delay period, we speculate possible
560 explanations for this as follows. Firstly, ALM neurons are involved in retaining working
561 memory related to future licking information in the delay period. When a tactile cue is given,
562 primary somatosensory cortex (vS1) encodes the tactile information and subsequently transfers
563 it to ALM (Guo et al., 2014). Also, medial motor cortex (MM) is activated in the sample period,
564 followed by the activation of ALM neurons in deep layers in the early delay period (Chen et
565 al., 2017). Hence, ALM neurons might become more coordinated as the delay period begins,
566 which would be likely to tighten the coupling of population activity of ALM neurons with the
567 shared space. Secondly, preparatory activities of motor cortical neurons stay on the null space
568 of movement execution to prevent muscle from evoking overt movements, thus coupling with
569 the shared space would also be changed after go cue (Guo et al., 2014; Stavisky et al., 2017;
570 Economo et al., 2018).

571 In this study, we showed that the selectivity of individual ALM neurons in mice varied with
572 the extent to which the neurons' firing activities were coupled to an intrinsic manifold shared
573 by the neurons. Our finding is in line with a recent computational study, which reported that a
574 latent state model based on recurrent neural networks could generate virtual neurons with
575 selectivity, suggesting that the selectivity of motor cortical neurons could be the result of latent
576 dynamics under which a population of neurons modulates their firing activities to perform a
577 task (Michaels et al., 2016). Yet, different from in-silico studies elucidating selectivity by latent
578 dynamics with synthetic neurons, the present study revealed that coupling to the intrinsic
579 manifold elucidated selectivity of biological ALM neurons.

580 Wei *et al.* showed similar dynamical structures underlying correct and erroneous behavior at
581 ALM population level (Wei et al., 2019). In their study, neural representations of population
582 activity in an intrinsic manifold reached toward the opposite direction during the error trials
583 but also hovered over intermediate areas between two possible licking directions. Consistent
584 with these results, we found less separable representations of population activities in the error
585 trials. However, different from this previous study's account of licking behavior based only on
586 neural representations of population activity in the intrinsic manifold, the present study
587 explains behavioral outcomes produced by individual neuronal firing characteristics
588 (selectivity) in association with latent structure (shared space).

589 The present study showed that the selectivity of individual ALM neurons could be partially
590 explained by the extent to which their firing activities were coupled to the intrinsic manifold
591 where the task-relevant information (i.e., licking direction) was manifested (see Figs. 7, 9).
592 This new account of selectivity may be applied to other similar neuronal activities found in
593 many brain areas such as preferred directions (Georgopoulos and Ashe, 2000; Omrani et al.,
594 2017) as well as other types of selectivity associated with various sensorimotor and cognitive
595 tasks (Rigotti et al., 2013; Amedi et al., 2017; Banerjee and Long, 2017).

596 Although biological implications of the shared space in the motor cortex remain elusive, many
597 studies have attempted to gain insights from the analysis of the shared space regarding task-
598 relevant neuronal population dynamics. For instance, studies have shown that the alignment of
599 an intrinsic manifold of wide-scale motor cortical neurons occurs in the course of task learning,
600 and the latent space becomes consolidated across neurons after learning (Ganguly et al., 2011;
601 Koralek et al., 2012; So et al., 2012; Koralek et al., 2013; Wander et al., 2013; Clancy et al.,
602 2014; Gulati et al., 2014). Also, a recent study suggests that anatomically separated cortical
603 areas interact with each other through the latent spaces (Semedo et al., 2019). Multiple brain

604 regions are reportedly involved together with ALM in the performance of the tactile delayed-
605 response task, including vS1, MM, thalamus, and cerebellum, implying that a large-scale
606 shared variance may emerge across multiple brain regions after learning to perform the task
607 (Li et al., 2016; Allen et al., 2017; Chen et al., 2017; Guo et al., 2017; Gao et al., 2018).

608 Dynamics underlying ALM selectivity can be described by a network model such as a discrete
609 attractor model (Inagaki et al., 2019) and possibly elucidate how erroneous behavior occurs
610 more precisely. But it is difficult to extend the network model to incorporate all inputs to ALM.
611 On the other hand, low-dimensional projection can effectively represent the task-relevant
612 variance of ALM neurons driven by input signals to ALM, because the projection methods such
613 as FA capture shared variance across neurons evoked by recurrence and input signals. For
614 example, the trajectory on the low-dimensional space of ALM showed ramping patterns similar
615 to those elicited by a ramping input from thalamus (Li et al., 2016; Inagaki et al., 2019). Thus,
616 in future studies, additional investigations are required to understand what aspect of neural
617 network dynamics is manifested the shared space. FA captures latent variables using covariance
618 among neurons, thus prominent inputs to ALM would be reflected on the covarying activities
619 of many ALM neurons, which is represented by latent factors. Considering that VM/VAL of
620 thalamus drives ALM dynamics, the shared space of ALM populations inferred by FA might
621 represent a subspace in which neuronal dynamics temporally evolve by strong thalamic inputs
622 (Guo et al., 2017). If thalamic feedback through the thalamocortical loop falsely draws
623 temporal growth of ALM activities to the fixed points corresponding to opposite licking
624 direction, then neural representation in the shared space would also change accordingly. In this
625 scheme, the selectivity of each ALM neuron would be altered depending on how much each
626 neuron is weighted by thalamic inputs, which would be described by communality in FA.

627

628 **References**

- 629 Allen WE, Kauvar IV, Chen MZ, Richman EB, Yang SJ, Chan K, Gradinaru V, Deverman BE,
630 Luo L, Deisseroth K (2017) Global Representations of Goal-Directed Behavior in
631 Distinct Cell Types of Mouse Neocortex. *Neuron* 94:891-907. e894.
- 632 Amedi A, Hofstetter S, Maidenbaum S, Heimler B (2017) Task Selectivity as a Comprehensive
633 Principle for Brain Organization. *Trends Cogn Sci* 21:307-310.
- 634 Athalye VR, Ganguly K, Costa RM, Carmena JM (2017) Emergence of Coordinated Neural
635 Dynamics Underlies Neuroprosthetic Learning and Skillful Control. *Neuron* 93:955-
636 970. e955.
- 637 Athalye VR, Santos FJ, Carmena JM, Costa RM (2018) Evidence for a neural law of effect.
638 *Science* 359:1024-1029.
- 639 Banerjee A, Long MA (2017) Ready, Steady, Go! Imaging Cortical Activity during Movement
640 Planning and Execution. *Neuron* 94:698-700.
- 641 Byron MY, Cunningham JP, Santhanam G, Ryu SI, Shenoy KV, Sahani M (2009) Gaussian-
642 process factor analysis for low-dimensional single-trial analysis of neural population
643 activity. In: *Adv Neural Inf Process Syst*, pp 1881-1888.
- 644 Chen TW, Li N, Daie K, Svoboda K (2017) A Map of Anticipatory Activity in Mouse Motor
645 Cortex. *Neuron* 94:866-879. e864.
- 646 Chen TW, Li N, Gerfen CR, Guo ZV, Svoboda K (2016) Calcium imaging responses from
647 anterior lateral motor cortex (ALM) neurons of adult mice performing a tactile decision
648 behavior.
- 649 Churchland MM, Shenoy KV (2007) Delay of movement caused by disruption of cortical
650 preparatory activity. *J Neurophysiol* 97:348-359.
- 651 Churchland MM, Cunningham JP, Kaufman MT, Ryu SI, Shenoy KV (2010) Cortical
652 preparatory activity: representation of movement or first cog in a dynamical machine?
653 *Neuron* 68:387-400.
- 654 Clancy KB, Koralek AC, Costa RM, Feldman DE, Carmena JM (2014) Volitional modulation
655 of optically recorded calcium signals during neuroprosthetic learning. *Nat Neurosci*
656 17:807.
- 657 Dempster AP, Laird NM, Rubin DB (1977) Maximum likelihood from incomplete data via the
658 EM algorithm. *J R Stat Soc Series B Stat Methodol* 39:1-22.
- 659 Economo MN, Viswanathan S, Tasic B, Bas E, Winnubst J, Menon V, Graybiel LT, Nguyen
660 TN, Smith KA, Yao Z (2018) Distinct descending motor cortex pathways and their roles
661 in movement. *Nature* 563:79.
- 662 Everett B (2013) *An introduction to latent variable models*: Springer Science & Business Media.
- 663 Ganguly K, Dimitrov DF, Wallis JD, Carmena JM (2011) Reversible large-scale modification
664 of cortical networks during neuroprosthetic control. *Nat Neurosci* 14:662.
- 665 Gao Z, Davis C, Thomas AM, Economo MN, Abrego AM, Svoboda K, De Zeeuw CI, Li N
666 (2018) A cortico-cerebellar loop for motor planning. *Nature* 563:113-116.

- 667 Georgopoulos AP, Ashe J (2000) One motor cortex, two different views. *Nat Neurosci* 3:963-
668 963.
- 669 Gulati T, Ramanathan DS, Wong CC, Ganguly KJNn (2014) Reactivation of emergent task-
670 related ensembles during slow-wave sleep after neuroprosthetic learning. *Nat Neurosci*
671 17:1107.
- 672 Guo ZV, Inagaki HK, Daie K, Druckmann S, Gerfen CR, Svoboda K (2017) Maintenance of
673 persistent activity in a frontal thalamocortical loop. *Nature* 545:181-186.
- 674 Guo ZV, Li N, Huber D, Ophir E, Gutnisky D, Ting JT, Feng G, Svoboda K (2014) Flow of
675 cortical activity underlying a tactile decision in mice. *Neuron* 81:179-194.
- 676 Inagaki HK, Inagaki M, Romani S, Svoboda K (2018) Low-Dimensional and Monotonic
677 Preparatory Activity in Mouse Anterior Lateral Motor Cortex. *J Neurosci* 38:4163-4185.
- 678 Inagaki HK, Fontolan L, Romani S, Svoboda K (2019) Discrete attractor dynamics underlies
679 persistent activity in the frontal cortex. *Nature* 566:212-217.
- 680 Koralek AC, Costa RM, Carmena JM (2013) Temporally precise cell-specific coherence
681 develops in corticostriatal networks during learning. *Neuron* 79:865-872.
- 682 Koralek AC, Jin X, Long JD, Costa RM, Carmena JM (2012) Corticostriatal plasticity is
683 necessary for learning intentional neuroprosthetic skills. *Nature* 483:331.
- 684 Li N, Gerfen CR, Svoboda K (2014) Extracellular recordings from anterior lateral motor cortex
685 (ALM) neurons of adult mice performing a tactile decision behavior.
- 686 Li N, Daie K, Svoboda K, Druckmann S (2016) Robust neuronal dynamics in premotor cortex
687 during motor planning. *Nature* 532:459-464.
- 688 Li N, Chen TW, Guo ZV, Gerfen CR, Svoboda K (2015) A motor cortex circuit for motor
689 planning and movement. *Nature* 519:51-56.
- 690 Michaels JA, Dann B, Scherberger H (2016) Neural Population Dynamics during Reaching
691 Are Better Explained by a Dynamical System than Representational Tuning. *Plos*
692 *Comput Biol* 12.
- 693 Omrani M, Kaufman MT, Hatsopoulos NG, Cheney PD (2017) Perspectives on classical
694 controversies about the motor cortex. *J Neurophysiol* 118:1828-1848.
- 695 Panzeri S, Harvey CD, Piasini E, Latham PE, Fellin T (2017) Cracking the Neural Code for
696 Sensory Perception by Combining Statistics, Intervention, and Behavior. *Neuron*
697 93:491-507.
- 698 Riehle A, Requin J (1989) Monkey primary motor and premotor cortex: single-cell activity
699 related to prior information about direction and extent of an intended movement. *J*
700 *Neurophysiol* 61:534-549.
- 701 Rigotti M, Barak O, Warden MR, Wang XJ, Daw ND, Miller EK, Fusi S (2013) The importance
702 of mixed selectivity in complex cognitive tasks. *Nature* 497:585-590.
- 703 Semedo JD, Zandvakili A, Machens CK, Yu BM, Kohn A (2019) Cortical Areas Interact
704 through a Communication Subspace. *Neuron* 102:249-259 e244.
- 705 So K, Ganguly K, Jimenez J, Gastpar MC, Carmena JM (2012) Redundant information

- 706 encoding in primary motor cortex during natural and prosthetic motor control. *J Comput*
707 *Neurosci* 32:555-561.
- 708 Stavisky SD, Kao JC, Ryu SI, Shenoy KV (2017) Motor Cortical Visuomotor Feedback
709 Activity Is Initially Isolated from Downstream Targets in Output-Null Neural State
710 Space Dimensions. *Neuron* 95:195-208. e199.
- 711 Tanji J, Evarts EV (1976) Anticipatory Activity of Motor Cortex Neurons in Relation to
712 Direction of an Intended Movement. *J Neurophysiol* 39:1062-1068.
- 713 Wander JD, Blakely T, Miller KJ, Weaver KE, Johnson L, A., Olson JD, Fetz EE, Rao RP,
714 Ojemann JG (2013) Distributed cortical adaptation during learning of a brain-computer
715 interface task. *Proc Natl Acad Sci U S A* 110:10818-10823.
- 716 Wang Y, Yin X, Zhang Z, Li J, Zhao W, Guo ZV (2021) A cortico-basal ganglia-thalamo-
717 cortical channel underlying short-term memory. *Neuron* 109:3486-3499 e3487.
- 718 Wei Z, Inagaki H, Li N, Svoboda K, Druckmann S (2019) An orderly single-trial organization
719 of population dynamics in premotor cortex predicts behavioral variability. *Nat Commun*
720 10:216.
- 721 Weinrich M, Wise SP, Mauritz KH (1984) A neurophysiological study of the premotor cortex
722 in the rhesus monkey. *Brain* 107 (Pt 2):385-414.
- 723
- 724

725 **Figure 1. Disruption of selective ALM activity tuned to the licking direction during**
726 **erroneous behavior**

727 **A.** A schematic diagram for the tactile delayed-response task. In the sample period, a
728 tactile cue represented as a pole position at either anterior or posterior whiskers was
729 given for 1.3 s to indicate the upcoming reward (water) direction. The anterior cue was
730 associated with the left direction whereas the posterior cue was with the right. Mice
731 should not move but wait during a 1.3-s delay period and began to lick toward either
732 the left or right direction after hearing an auditory go cue.

733 **B.** Four possible behavioral results from the delayed-response task depending on the
734 match between the tactile cue (anterior vs. posterior) and licking direction (left vs.
735 right): hit left (HL); error right (ER); error left (EL); and hit right (HR). Error right (left
736 denotes erroneous movement to the left (right) given a right-directing (left-directing)
737 cue.

738 **C.** No significant difference in the behavioral performance of the tactile delayed-response
739 task between licking directions ($p > 0.1$, two-tailed paired t -test, $n = 22$). Error bars,
740 s.e.m. across the mice.

741 **D.** Examples of the selective firing activities (i.e., selectivity) of three representative ALM
742 neurons when mice performed the tactile delayed-response task, for each of the four
743 cases of behavioral outcomes (HL, HR, ER and EL). Each neuron showed peak activity
744 in a particular period when the task goal (left or right direction) agreed with its
745 selectivity (left or right) and when mice behaved correctly (HL and HR). This selective
746 firing activity became more ambiguous when mice behaved wrongfully (ER and EL).
747 Also, differences in activities between HR and HL in a particular period were large in
748 the hit trials (top), which was less apparent in the error trials (bottom).

749 **E.** Differences in the firing activity of the ALM neurons showing selectivity between
750 licking directions. Contra-preferring neurons denote the ALM neurons with selectivity
751 to the right direction (note: left ALM neurons were recorded) and ipsi-preferring
752 neurons do for the left direction. Differences in firing activities of these neurons
753 between licking directions were shown in the hit and error trials, based on the fold
754 changes from baseline activity ($*p < 0.05$, $**p < 0.01$, Bonferroni-corrected *post-hoc*
755 test). While the neurons exhibited significant differences between the directions for
756 every period in the hit trials (left), such differences mostly disappeared in the error
757 trials (right). Error bars, s.e.m. across the neurons.

758

759 **Figure 2. Changes in selectivity of ALM neurons between correct and erroneous behavior**

760 **A.** Distributions of selectivity in the correct (hit) and erroneous (error) trials for each
761 period (sample, delay and response). Black dots represent individual neuronal
762 selectivity in the hit and the error trials. Gray lines connecting each pair of the black
763 dots indicate the selectivity change of the corresponding neuron between the hit and
764 error trials. The vertically oriented shadings indicate the sample distributions of
765 selectivity for hit (gray) or error (pink) trials, respectively. While individual neuronal
766 selectivity was decreased or increased across the hit and error trials, there was no
767 significant difference in the distribution of the selectivity between the hit and error
768 trials (K-S test, $p > 0.05$) for every period.

769 **B.** 10% of the ALM neurons, marking the top 5% contra-preferring and the top 5% ipsi-
770 preferring selectivity in the hit trials (black dots), significantly decreased their
771 selectivity in the error trials (red dots) for every period (one-tailed paired t -test, $p < 10^{-6}$).
772 The gray lines indicate selectivity changes between hit and error trials of each
773 neuron.

774 **C.** 10% of the ALM neurons, marking the top 5% contra-preferring and the top 5% ipsi-
775 preferring selectivity in the error trials (black dots), significantly decreased their
776 selectivity in the hit trials (red dots) for every period (one-tailed paired t -test, $p < 0.01$).
777 The gray lines indicate selectivity changes between hit and error trials of each neuron.

778

779 **Figure 3. Reversed firing modulation of ALM neurons**

780 **A.** The schematic diagram illustrating reversed firing modulation (see Methods). If
781 (hypothetic) neurons decrease firing rates in the error trials in response to a preferred cue
782 that originally increases the firing rates in the hit trials and vice versa, neurons are deemed
783 to exhibit reversed firing modulation. For example, with reversed firing modulation,
784 neurons that show higher firing rates for correct right licking (HR) than for correct left
785 licking (HL) would decrease firing rates in response to a right directional cue for erroneous
786 left licking (ER) (left) while increase firing rates in response to a left directional cue (EL)
787 (middle). If two neurons with similar selectivity exhibit reversed firing modulation, their
788 firing rates would be correlated even over the error trials as well as over the hit trials (right).

789 **B.** Examples of correlated firing rates of two ALM neurons showing reversed firing
790 modulation. In the hit trials, two contra-preferring neurons (neurons #3 and #10, session
791 ALM219031) similarly increased firing rates when the posterior cue was given, showing a
792 high correlation ($r = 0.85$) between their firing rates over the hit trials (left). But in the error
793 trials, both neurons increased firing rates when the anterior cue was given, such as ipsi-
794 preferring neurons, showing again a high correlation ($r = 0.81$) over the error trials (middle).
795 Yet, such a correlation disappeared in the error trials when the trial order was shuffled
796 (right).

797 **C.** Correlations between neurons showing reversed firing modulation. Pearson correlation
798 coefficient was calculated between all pairwise combinations of the neurons showing
799 reversed firing modulation (see Methods for the criterion to determine a neuron with
800 reversed firing modulation) for the hit and error trials, respectively, in each period. The
801 average correlation coefficient was not significantly different between the hit and error
802 trials (two-tailed paired t -test, $p > 0.1$) in the delay and response periods, or greater over

803 the error trials than over the hit trials in the sample period (one-tailed paired t -test, sample:
804 $p < 0.05$). N denotes the total number of neurons showing reversed firing modulation
805 summed over the sessions. $Pair$ denotes the sum of the number of all possible pairs of such
806 neurons calculated session-wise (e.g., if $N=2$ in Session 1 and $N=3$ in Session 2, then $Pair$
807 $= {}_2C_2 + {}_3C_2 = 5$). Note that N and $Pair$ should remain the same across the hit and error trials
808 in a given period. Error bars, s.e.m. across pairs.

809

810 **Figure 4. Neural representations of task-relevant information in the shared space of ALM**
811 **neurons**

812 **A.** Examples of the task-related information representation in the shared space composed
813 of the latent variables 1 and 2 (LV1 and LV2) (top: hit trials, bottom: error trials). Each
814 dot represents the 2D values of the latent variables resulting from the factor analysis of
815 the firing rates of ALM population at each trial. In the hit trials, the latent variables
816 (especially LV1) distinctly represented the target direction information (HR or HL) in
817 all the periods, which became less apparent in the error trials.

818 **B.** The Fisher ratio between the two groups of the values corresponding to each target
819 direction was calculated for each latent variable (LV1 and LV2), and compared among
820 the hit, error and randomly shuffled trials (ANOVA, $*p < 0.05$, $**p < 0.01$, Bonferroni-
821 corrected *post-hoc t*-test). Randomly shuffling was performed for the hit trials. Error
822 bars, s.e.m. across sessions.

823 **C.** The schematic diagram for illustrating the testing of consistent emergence of task-
824 related information in the shared space (see Methods for detailed descriptions). A
825 shared space is first built using HIT_{train} data, followed by the projection of HIT_{test} data
826 onto that shared space (HIT_{train} data: ALM neurons' firing rate data from a part of the
827 hit trials used for training the factor analysis model; HIT_{test} : ALM neurons' firing rate
828 data from the remaining hit trials not used for training). Whether the representation of
829 task-related information in the shared space is consistent throughout the trials is
830 evaluated by two distances: 1) same-cue distance (left; between the same cues) and 2)
831 opposite-cue distance (right; between the different cues). Distance is measured by the
832 Fisher ratio between the two groups of the latent variable values corresponding to the
833 train and test data, respectively (for LV1 and LV2 each). If the shared space consistently

834 represents the target direction information across trials, then the same-cue distance
835 would remain small while the opposite-cue distance would remain large between
836 HIT_{train} and HIT_{test} . This test is also applied between HIT_{train} and ERR_{test} , where ERR_{test}
837 indicates ALM neurons' firing rate data from the error trials.

838 **D.** Examples of the task-related information represented in the shared space. As a standard,
839 HIT_{train} was projected onto the shared space built using the same data of HIT_{train} (top).
840 Each dot represents the projection outcome in each trial. HIT_{test} and ERR_{test} were
841 projected onto the shared space constructed by HIT_{train} , respectively (middle and
842 bottom).

843 **E.** The same-cue and opposite-cue distances measured by the Fisher ratio for each latent
844 variable (LV1 and LV2) in each period. First, the opposite cue distance using HIT_{train}
845 only was measured as the standard distance value (black). Then, the same-cue and
846 opposite-cue distances were measured for HIT_{test} (grey) and ERR_{test} (red), respectively.
847 Note that the opposite-cue distance using HIT_{train} only was measured by the Fisher ratio
848 of HIT_{train} on the shared space built using the same HIT_{train} . Each of the same-cue and
849 opposite-cue distances was compared with the standard distance value (one-tailed
850 paired t -test), $*p < 0.05$, $**p < 0.01$). Error bars, s.e.m. across sessions.

851

852 **Figure 5. Selectivity in firing rates and shared signals of ALM neurons**

853 **A.** Venn Diagrams of the number of neurons showing selectivity in each period. FR+
854 denotes the neurons that have selectivity in firing rates (top: contra-preferring neuron;
855 bottom: ipsi-preferring neuron). FR+SH+ denotes then neurons that have selectivity in
856 both firing rates and shared signals (see Methods for the description of the shared
857 signal of a neuron).

858 **B.** For the FR+SH+ neurons, selectivity in shared signals (S_{elSH}) is greater in magnitude
859 than selectivity in firing rates (Selectivity) in every period (top, one-tailed paired t -test,
860 $p_s < 0.05$ for every period). Linear regression of Selectivity against S_{elSH} yielded
861 significant linear fits (bottom, $p_s < 0.05$), with every slope < 1 in each period.

862

863 **Figure 6. Alteration of selectivity in erroneous behavior is related to alteration of latent**
864 **variables while relations between firing rates and latent variables are unchanged**

865 **A.** The scatter plots of reconstructed Sel_{SH} and original Sel_{SH} in the hit trials. Each dot
866 denotes each session. Reconstructed Sel_{SH} was the selectivity of the shared signals
867 reconstructed by the loading matrix (U) obtained from the hit trials and latent variables
868 (z) obtained from the error trials. A significant correlation was observed between
869 reconstructed Sel_{SH} and original Sel_{SH} only in the delay period ($p < 0.01$), where the
870 correlation coefficient was negative ($r = -0.33$). The negative correlation indicates that
871 z in the error trials were reversely formed, thus generating altered selectivity (see the
872 text for more details).

873 **B.** The scatter plots of reconstructed Sel_{SH} and original Sel_{SH} in the hit trials. Different
874 from A, the shared signals were now reconstructed using U obtained from the error
875 trials and z from the hit trials. For every period, reconstructed Sel_{SH} and original Sel_{SH}
876 were positively correlated ($ps < 0.01$).

877

878 **Figure 7. Selectivity of individual neurons is positively correlated with their communality**
879 **to the shared space**

880 **A.** Correlations between communality and selectivity in the hit trials. The communality
881 and selectivity across individual neurons were positively correlated in every period (r ,
882 Pearson's correlation coefficient, $**p < 0.01$).

883 **B.** The scatter plots of communality and selectivity across individual neurons in the hit
884 trials. The dashed lines indicate significant regression lines obtained from linear
885 regression ($ps < 0.01$). Each circle reflects a single neuron. Note that selectivity was
886 normalized before calculating correlations to compare the differences between neurons
887 regardless of the session.

888 **C.** Correlations between communality and selectivity in error trials. No significant
889 correlation was observed in any period ($ps > 0.1$).

890 **D.** The scatter plots of communality and selectivity across individual neurons in the error
891 trials. Linear regression revealed no significant linear relationships between
892 communality and selectivity ($ps > 0.1$). Each circle reflects a single neuron.

893

894 **Figure 8. Changes in communality between correct and incorrect behavior**

895 **A.** Distributions of communality in the correct (hit) and erroneous (error) trials for each
896 period (sample, delay and response). Black dots reflect the communality of single
897 neurons in the hit and the error trials. Gray lines connecting each pair of dots between
898 the hit and error trial indicates communality change of the corresponding neuron
899 between the hit and error trials. The vertically oriented shadings indicate sample
900 distributions of selectivity for hit (gray) or error (pink) trials, respectively. The K-S test
901 showed that the cumulative density function of communality in the hit trials was
902 significantly smaller than that in the error trials ($ps < 10^{-4}$ for every period).

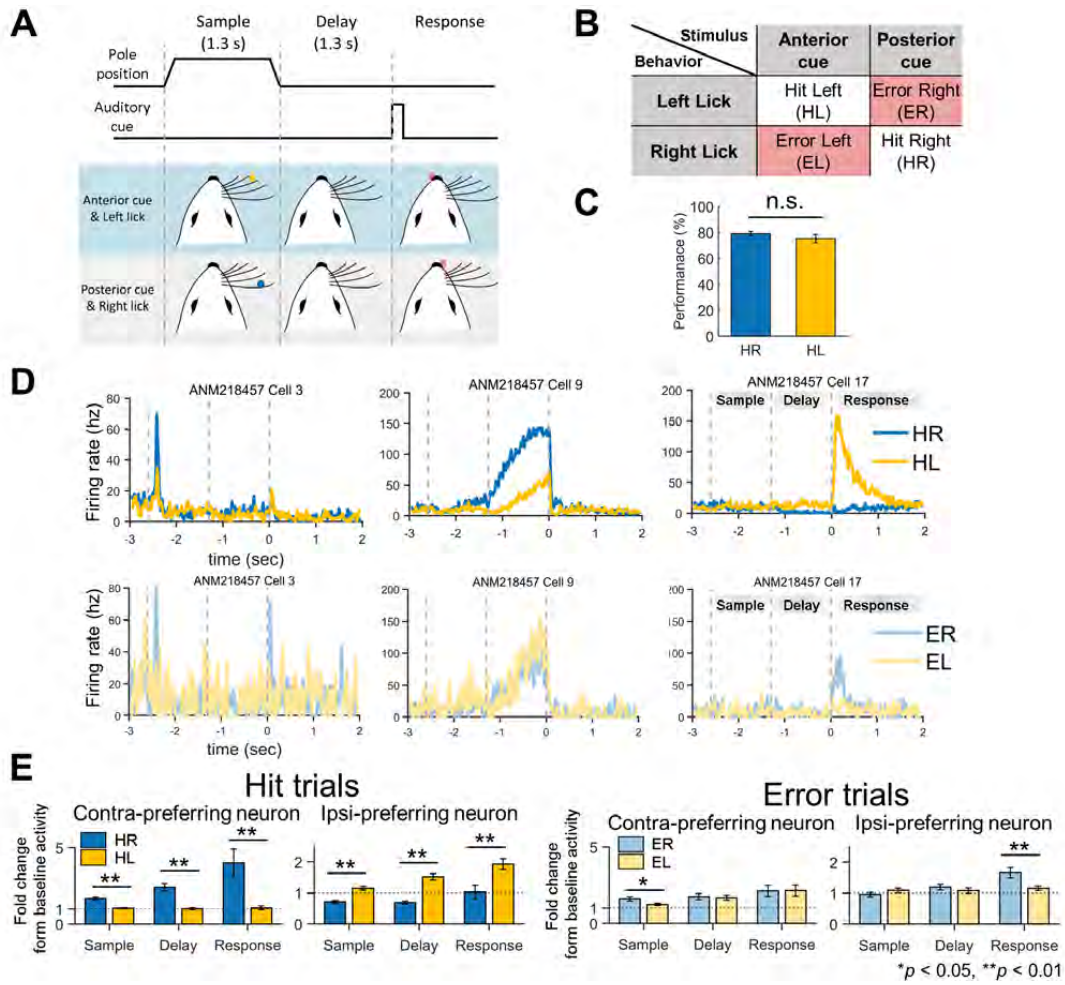
903 **B.** Neurons with the top 10 % highest communality in the hit trials significantly decreased
904 their communality in the error trials for every period (one-tailed paired t -test, $p < 0.01$).
905 Gray lines indicate communality changes from the hit to the error trials of single
906 neurons.

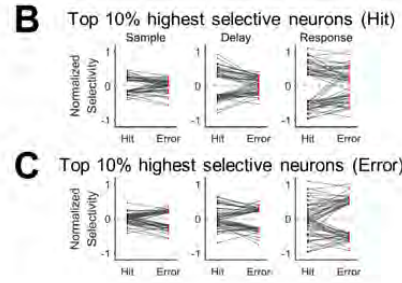
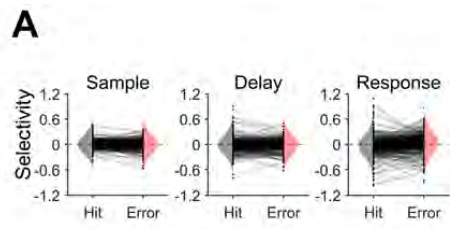
907 **D.** Neurons with the top 10% highest communality in the error trials significantly
908 decreased their communality in the hit trials for every period (one-tailed paired t -test,
909 $p < 0.01$). Gray lines indicate communality changes from the hit to the error trials of
910 single neurons.

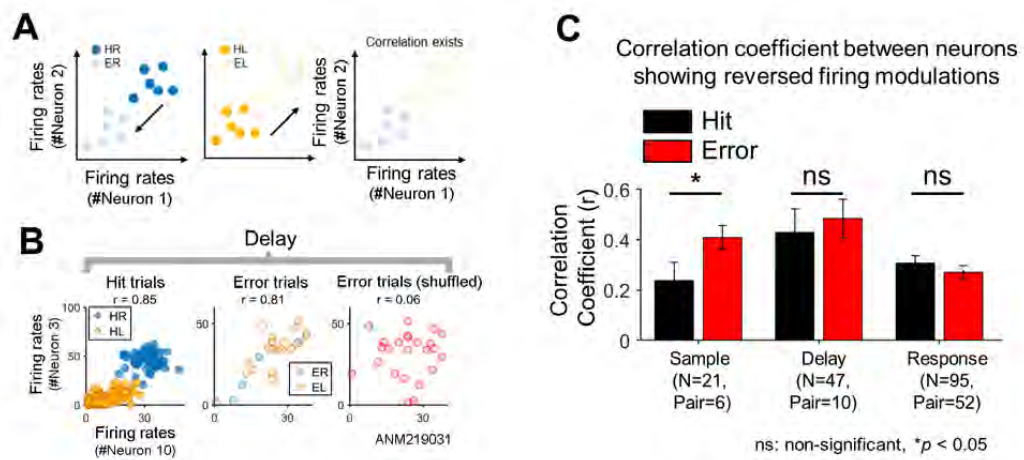
911 **Figure 9. Altered selectivity of ALM neurons with motor planning error is related to**
912 **altered communality**

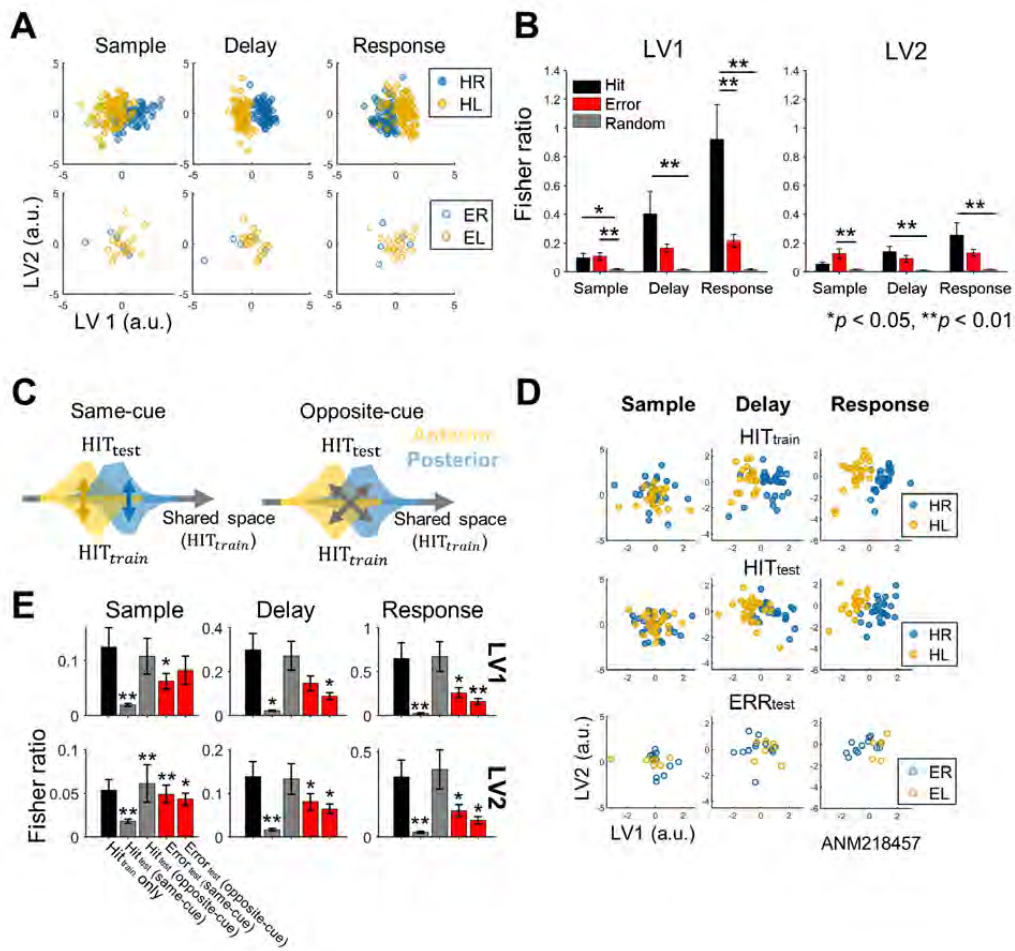
913 **A.** Correlations between the mean communality change and the mean selectivity change
914 from the hit to the error trials, where the mean was estimated over the population of
915 neurons in each session, were calculated across sessions (r , Pearson's correlation
916 coefficient). A significant correlation was observed only in the delay period (** $p <$
917 10^{-3}).

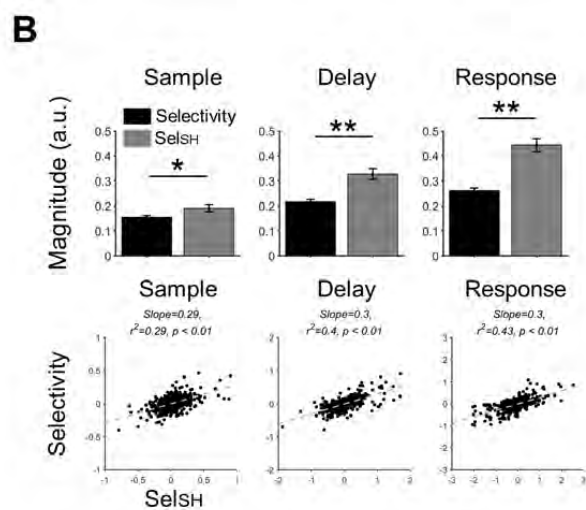
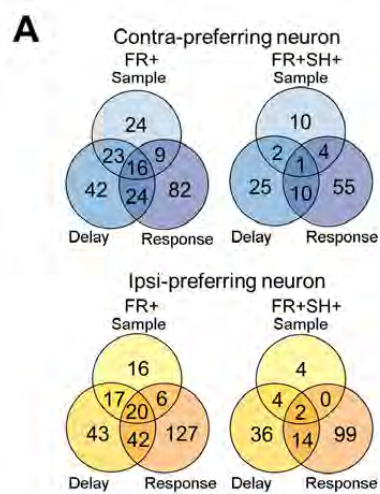
918 **B.** The scatter plots of the mean communality differences and the mean selectivity
919 differences in each period. Each dot reflects each session. The dashed regression line
920 was obtained from linear regression ($p < 0.01$).

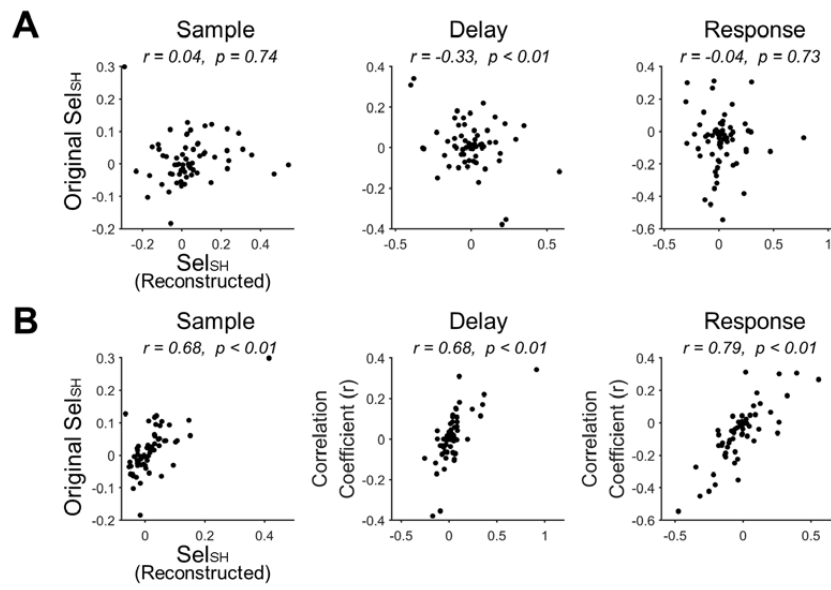


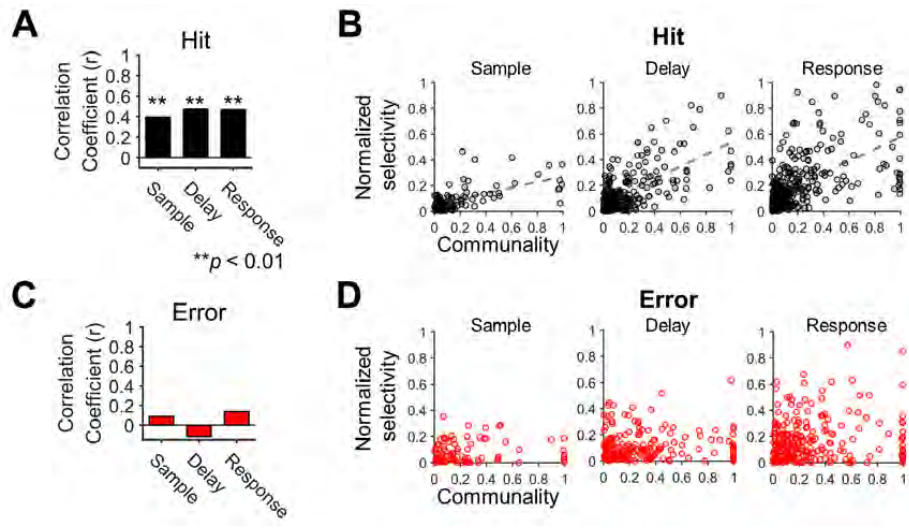




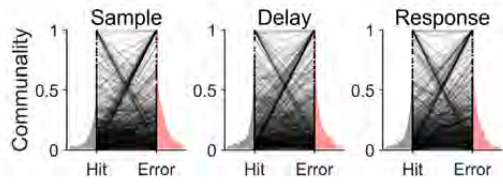




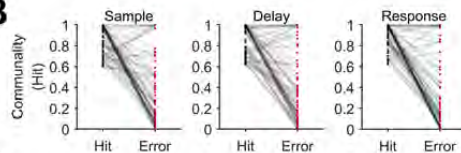




A



B



C



